Heat Transfer at the Subcooled-Scraped Surface with/without Phase Change

Frank G. F. Qin, Xiao Dong Chen, and Andrew B. Russell
Dept. of Chemical and Materials Engineering, The University of Auckland, Auckland, New Zealand

Continuous heat extraction is important for the process of freeze concentration of aqueous solutions, in which water is removed as solid ice. Three typical unsteady heat transportation patterns were distinguished at the subcooled surface of a scraped-surface heat exchanger (SSHE) in this study. They were found in different stages of freeze concentration. Experimental measurement of the heat-transfer coefficient in an SSHE showed that the overall heat-transfer coefficient of stage III, which was characterized by ice formation on the cooler surface, was about 1.5 times higher than stage I, where no ice formed. Although the ice layer (also known as ice fouling) on a heat exchanger surface may be considered disadvantageous for heat transfer, the initial ice formation actually "boosted up" the heat transportation in an SSHE. The mechanism analysis and mathematical modeling of this phenomenon, however, have not been found in the literature. A mathematical model is developed and a unified expression of the heat-transfer coefficient in an SSHE with/without phase change is presented. The model predicts a step increase of heat transfer occurs at the onset of ice formation and the maximum heat-transfer coefficient exists in a narrow range right after reaching the freezing point. These are consistent with the experimental results of this study.

Introduction

Aqueous solution in contact with the scraped-subcooled metal surface will be subjected to three heat-transfer stages: chilling, nucleation, and freeze concentration. Liquid becomes more viscous when its temperature gets lower, and ice cake can form when the liquid starts to freeze. In the food industry, surface scraping can be used on the subcooled metal surface in order to maintain the heat-transfer efficiency by removing the ice layers. Applications can be found in the production of ice cream and in the ice nucleator of freeze concentration, etc. A general expression of overall heat-transfer coefficient U can be written as

$$\frac{1}{U}=\frac{1}{h_c}+\frac{b}{\lambda_w}+\frac{1}{h_l}+\frac{\epsilon}{\lambda_f}, \tag{1}$$

where h_c, h_l are the individual heat-transfer coefficients of the coolant and the food liquid, respectively; λ_w, λ_f are the thermal conductivities of the wall material and the fouling layer, respectively; b, ϵ are the thicknesses of the wall and fouling layer, respectively. In many industrial circumstances the heat-transfer rates are predominated by the heat-transfer coefficient h_l of the liquid film and the heat-transfer resistance, ϵ/λ_f, of the fouling layer. Therefore scraped-surface heat exchangers (SSHE) are used for high viscous or particulate materials to improve the operating performance (Abichandani et al., 1987). Although the theory and practice of SSHE have been widely studied by many researchers for different applications (Cuevas et al., 1982; Harrod, 1986; Abichandani et al., 1987; Djelveh and Gros, 1995; Chandarana and Unverferth, 1996; Baccar and Abid, 1997), the behavior of heat transfer in low Reynolds number of viscous fluids, especially when a dynamic phase change (crystallization) is involved on the subcooled scraped surface, has not been fully studied. A comprehensive model to describe this process is not yet available in the literature. In this study, attention has been given to the experimental analysis and the modeling of the individual heat-transfer coefficient, h_l, and the dynamic heat-transfer resistance of the ice fouling on the scraped subcooled surface.

Correspondence concerning this article should be addressed to X. D. Chen.
Current address for A. B. Russell: Unilever R&D Coluworth, Sharnbrook Bedford, U.K.

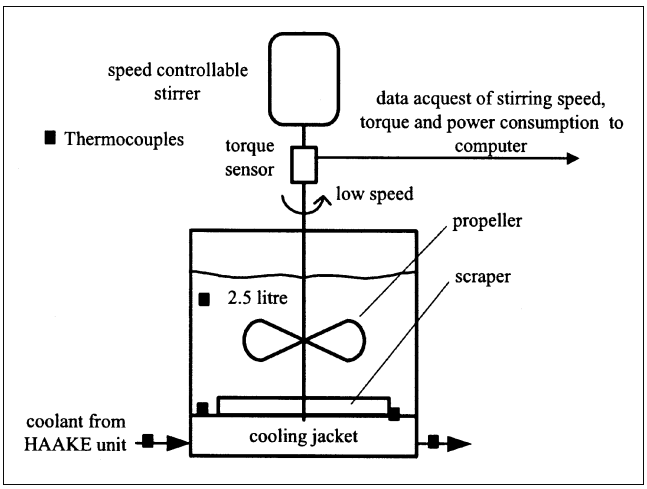

Figure 1. Experimental setup.

Experimental

Apparatus and methods

The experiments were carried out in a cylindrical vessel with a cooling jacket at the bottom, shown by Figure 1. A group of thermocouples were placed at the appropriate points to measure the cooling surface, bulk solution, and cooler inlet and outlet temperatures. The data were recorded using Picologger (Pico Technology Ltd., UK) connected to a PC. The bulk temperature was controlled by coolant circulation, which was provided by a HAAKE unit (Gebruder HAAKE GmbH., Germany). The solution was agitated by a stirrer. The stirring shaft also carried a scraper with two blades to provide surface scraping on the jacket wall. The stirrer speed was set at 100 rpm. The exterior of the vessel was insulated to minimize heat loss.

The milk in the vessel was first chilled from room temperature to a low temperature before ice formation. No phase change occurred during this period. The temperature difference for heat transfer mainly fell on the interface of the coolant and the jacket wall because both bulk agitation and surface scraping were used on the milk side at the speed of 100 rpm. This is shown in Figure 2 in segment I of the temperature–time curves. The bulk temperature almost linearly decreased when the coolant temperature was kept constant (Figure 2a), or changed linearly with time (Figure 3a). The overall heat-transfer coefficient in stage I can be determined by measuring the variation of bulk temperature. The energy balance at an arbitrary moment t from the liquid (10 wt % whole milk in this study) to the coolant is expressed as

$$dQ_1 = U_I A(T_m - T_c)\, dt, \tag{2}$$

where U_I is the overall heat-transfer coefficient in stage I; A is the surface area of the cooling jacket (0.02269 m^2 in this study); and T_m and T_c are the milk temperature and coolant temperature, respectively. The milk temperature is a function of time, $T_m(t)$, during the chilling period, which can be determined experimentally. The coolant temperature, T_c, is the average value of the inlet and outlet temperatures.

If the temperature of the milk in the vessel decreases from T_{m1} to T_{m2} during this time interval from t_1 to t_2, the heat

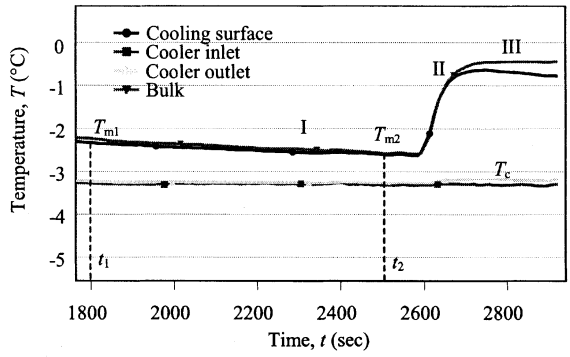

(a) Temperature variation of the system in three different stages

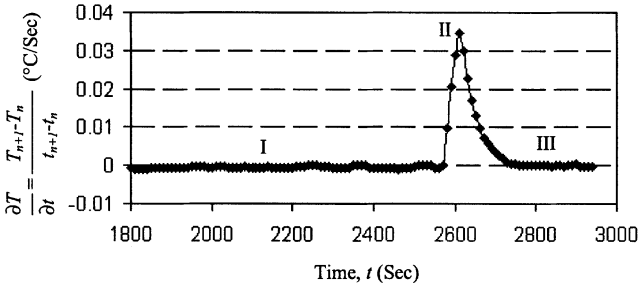

(b) Numerical differential of bulk temperature against time

Figure 2. Three heat-transfer patterns on a sub-cooled-scraped metal surface with fixed coolant temperature.

removed is

$$Q_2 = \rho_l c_{pl} V(T_{m1} - T_{m2}), \tag{3}$$

where ρ_l and c_{pl} are the density and specific heat of the liquid (which is whole milk in this study); they are 1,060 $kg \cdot m^{-3}$ and 3,910 $J \cdot kg^{-1} \cdot °C^{-1}$, respectively. Thermal insulation with the environment gives the heat balance of $Q_1 = Q_2$, and this leads to

$$U_I = \frac{\rho_l c_{pl} V(T_{m1} - T_{m2})}{A\int_{t_1}^{t_2}(T_m - T_c)\, dt}, \tag{4}$$

where the integral bound is from t_1 to t_2; t_1 and t_2 correspond to the time when the bulk temperatures, T_{m1} and T_{m2}, respectively, were measured (Figure 2a).

The temperature increased rapidly in stage II because of the onset of ice nucleation, which can be found in Figures 2a and 3a. The latent heat of freezing raised the bulk temperature to approximately the freezing point of the milk, which was about -0.5°C for whole milk at the solids content of 10 wt %. The bulk temperature in stage III was very stable. It almost stays at its freezing point. A slight decrease of bulk temperature in stage III was the result of freezing-point depression of the milk due to freeze concentration.

The overall heat-transfer coefficient, U_{III}, in the third stage can be determined by measuring the concentration increase of the milk in a definite time. If the original milk mass and

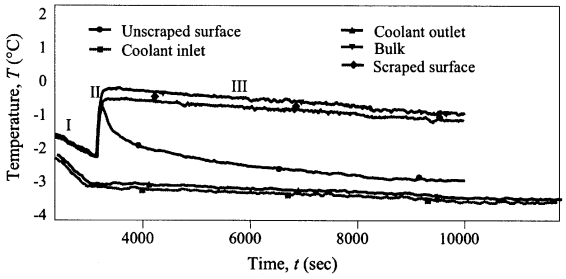

(a)Temperature variation of the system during the process of freeze concentration

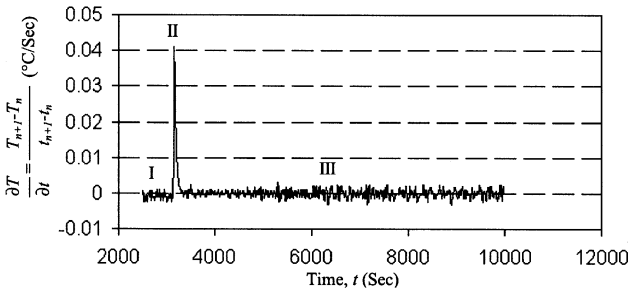

(b)Numerical differential of the bulk temperature against time

Figure 3. Three typical heat-transfer patterns found at subcooled SSHE with varying coolant temperature in stage I and fixed coolant temperature in stage III.

solid content are M_m and C_1, respectively, C_2 is the final solid content after freeze concentration. At the end of the operation, the mass of water that has been frozen in ice is

$$M_{\text{ice}} = M_m\left(1 - \frac{C_1}{C_2}\right) \tag{5}$$

So the total latent heat liberated by ice formation is $Q_1 = \Delta H_i M_{\text{ice}} = \Delta H_i M_m(1 - C_1/C_2)$. And the total heat transferred through the cooling surface is $Q_2 = AU_{\text{III}} \cdot (T_m - T_c) \cdot t$. Since Q_1 equals Q_2, this leads to

$$U_{\text{III}} = \frac{\Delta H_i M_m}{A(T_m - T_c)t}\left(1 - \frac{C_1}{C_2}\right) \tag{6}$$

Here, U_{III} is the overall heat-transfer coefficient in the third stage; ΔH_i is the latent heat of freezing of water; and t is the operation time of freeze concentration.

Data acquisition of the computer system provides another method for analyzing the experimental results: the numerical differential of temperature against time based on the logged numerical data. This gives the rate of temperature variation with time, which is, geometrically, the slope of the temperature–time curve at the instant of time t_n

$$\left.\frac{\partial T}{\partial t}\right|_{t=t_n} = \frac{T_{n+1} - T_n}{t_{n+1} - t_n}, \tag{7}$$

where $T_{n+1} - T_n$ is the temperature difference at a short time interval between t_{n+1} and t_n.

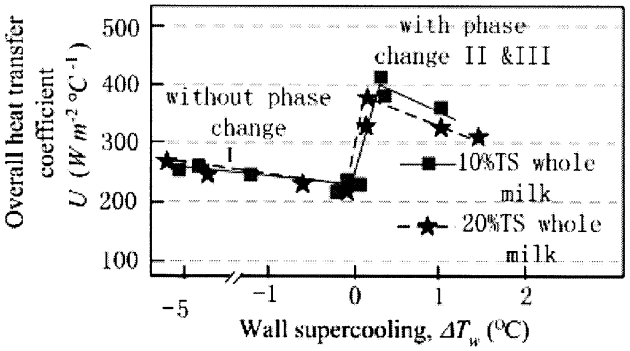

Figure 4. Measured heat-transfer coefficients have a step increase when ice formation occurs at the subcooled SSHE, and achieve a maximum at a low degree of supercooling.

Experimental results and discussions

The overall heat-transfer coefficient, U_{I}, of stage I was found to be 275 ($\text{Wm}^{-2}\cdot\text{°C}^{-1}$) in the equipment used in this study according to Eq. 4. As a comparison, the overall heat-transfer coefficient, U_{III}, in stage III, shown in Figure 3a, was found to be 415 ($\text{Wm}^{-2}\cdot\text{°C}^{-1}$) according to Eq. 6, which is about 1.5 times larger than U_{I} of stage I. This means the ice growth on the cooling surface, which might lead to ice fouling, actually "boosts up" the heat transfer if the newly formed ice can be removed continuously (Figure 4). The mechanism of this process, however, hasn't been fully explained, though it is generally believed that this is caused by the direct liberation of the latent heat of ice crystallization at the subcooled surface (Zheng et al., 2001). The mathematical model of heat transfer for this process hasn't been seen in the literature.

Numerical differential of temperature against time $\partial T/\partial t$ in Figures 2a and 3a were given in Figures 2b and 3b, respectively. Note the temperature changing rate in stages I and III is very close to zero, that is, $(\partial T/\partial t)_{\text{I}} \approx 0$ and $(\partial T/\partial t)_{\text{III}} \approx 0$, implying that the heat transfer over the entire scraped surface on a time-average base is a quasi-steady-state in both of them, though the heat transfer on a small area of the element is unsteady within the time interval of a scraped circle. This conclusion will be used later for establishing the mathematical model of the heat transfer in stage III, in which phase change on the subcooled scraped surface is involved.

Mathematical Modeling

Heat transfer on the scraped surface without phase change (stage I)

In stage I, where no ice is formed on the cooling surface, the heat flux can be treated as a one-dimensional condition. After the scraping action on the cooling surface, the solution has a uniform bulk temperature (T_b), which gives the initial condition of Eq. 9. Here the initial time is defined as the moment when a scrape blade has just wiped over the cooling surface. We assume that the liquid boundary layer is completely replaced by bulk solution. After this moment, the solution temperature at the cooling surface quickly drops to the wall temperature (T_w) and is held until the next blade wipes over. We also assume that the coolant flow is sufficient

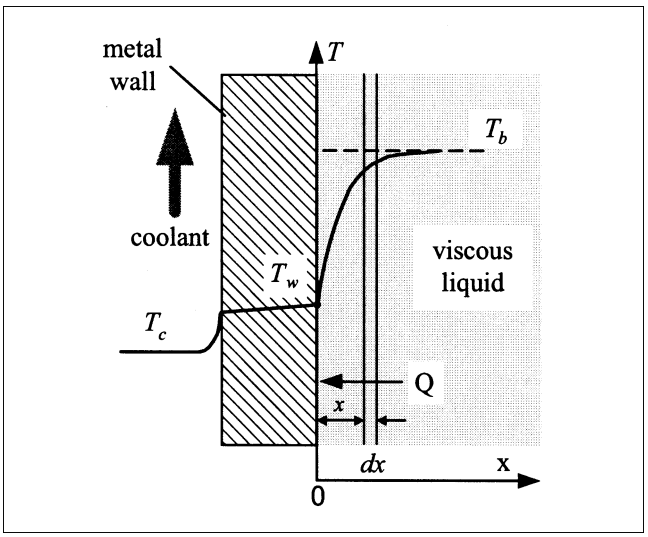

Figure 5. Heat transfer above the scraped cooling surface.

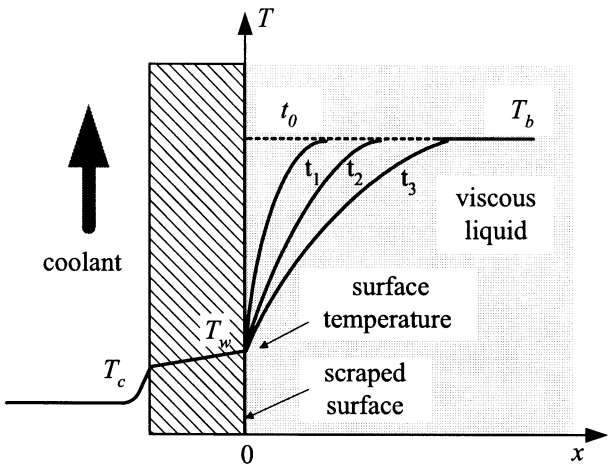

Figure 6. Temperature profile at different times after the action of scrape.

enough to maintain a constant wall temperature (T_w). This will give the boundary condition of Eq. 10. In the remote distance, the bulk temperature will always remain at T_b, which leads to a semi-infinite condition expressed by Eq. 11.

Look at the thin layer of thickness dx located at distance x from the metal wall, as shown in Figure 5. The following heat balance can be recognized

$$\text{Heat flow into the layer} - \text{Heat flow out of the layer} = \text{Heat accumulation in the layer}$$

This leads to the establishment of a one-dimensional heat-transfer Eq. 8 (Holman, 2002)

$$\begin{cases} \dfrac{\partial T}{\partial t} = \alpha_l \dfrac{\partial^2 T}{\partial x^2} & (8) \\ T(x,0) = T & (9) \\ T(0,t) = T_w & (10) \\ T(\infty,t) = T_b, & (11) \end{cases}$$

where $\alpha_l = \lambda_l/\rho_l c_{pl}$ is known as the thermal diffusivity and is a property of the cooled liquid.

Let $\theta = (T - T_w)/(T_b - T_w)$. An analytical solution of this problem can be expressed with the error function

$$\frac{T - T_w}{T_b - T_w} = \frac{2}{\sqrt{\pi}} \int_0^z e^{-z^2} dz, \qquad (12)$$

where $z = x/2\sqrt{\alpha_l t}$; x is the distance from the cooling surface; t is the time elapsed after the scraping action. Derivation of the solution (Eq. 12) is detailed in the Appendix. Figure 6, a schematic diagram of the temperature profile according to Eq. 12, shows the specific instant of time, t_1, t_2, t_3, after the blade passes over.

This solution is used to find the expression of the heat-transfer coefficient of the SSHE. The temperature gradient at the cooling surface ($x = 0$) is found by differentiating Eq. 12 against x, giving

$$\frac{\partial T(0,t)}{\partial x} = \frac{T_b - T_w}{\sqrt{\pi \alpha_l t}}. \qquad (13)$$

The heat flux at the cooling surface is related to the temperature gradient by Fourier law

$$\left.\frac{\partial Q}{\partial t}\right|_{x=0} = -\lambda_l A \left(\frac{\partial T}{\partial x}\right)_{x=0} = -\frac{\lambda_l A (T_b - T_w)}{\sqrt{\pi \alpha_l t}}, \qquad (14)$$

where the minus sign denotes that the heat flux is opposite to the direction of the temperature gradient (similarly hereinafter). From the beginning of the scrape action ($t = 0$) to a certain instant of time ($t = \tau$), the heat extracted from the liquid to the cooling surface can be obtained by integrating Eq. 14 from the time of $t = 0$ to $t = \tau$

$$|Q_\tau| = \frac{\lambda_l A (T_b - T_w)}{\sqrt{\pi \alpha_l}} \int_0^\tau \frac{dt}{\sqrt{t}} = 2\lambda_l A (T_b - T_w) \left(\frac{\tau}{\pi \alpha_l}\right)^{1/2}. \qquad (15)$$

During the period of $0-\tau$, the average heat-transfer coefficient is, by definition

$$\bar{h}_l = \frac{|Q_\tau|}{A(T_b - T_w)\tau}. \qquad (16)$$

Substitution of Eq. 15 into Eq. 16, noting $\alpha_l = \lambda_l/\rho_l c_{pl}$, gives

$$\bar{h}_l = \frac{2\lambda_l}{\sqrt{\pi \alpha_l \tau}} = 2\left(\frac{\lambda_l \rho_l c_{pl}}{\pi \tau}\right)^{1/2}, \qquad (17)$$

where λ_l is the thermal conductivity of the liquid, and τ is the interval time between two scrape actions. If scraping is

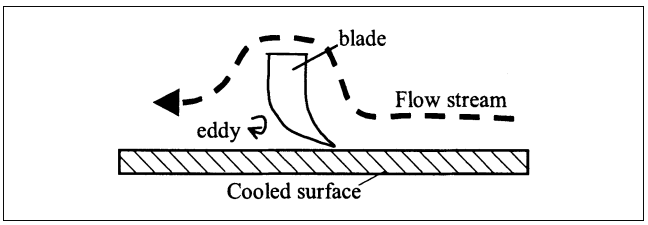

Figure 7. Portion of liquid may return to the cooling surface.

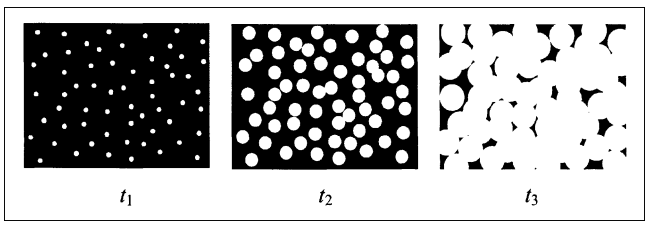

Figure 8. Initial period of ice nucleation and growth on the subcooled metal surface, where white spots represent ice patch, black area represents the metal surface.

carried out by rotation, either on a cylindrical or a round-dish surface, the time interval is

$$\tau = \frac{60}{nF} \text{ (s)}, \tag{18}$$

where n is the rotational speed, rpm, and F is the number of blades carried by the shaft. Combining Eqs. 18 and 17 yields

$$\bar{h}_l = \left(\frac{\lambda_l \rho_l c_{pl} nF}{15\pi} \right)^{1/2}. \tag{19}$$

Note that here the heat-transfer coefficient $\bar{h}_l$ is a time average over a scrape circle. This model shows that the heat-transfer coefficient $\bar{h}_l$ is impacted by the thermal properties of the liquid (λ_l, ρ, and c_p) and the scrape strength (that is, the product of rotational speed, n, and blade number, F), but has nothing to do with the viscosity of the liquid. This is because we have assumed that the liquid layer on the cooling surface is completely removed by the scraper, and this liquid will fully mix with the bulk. The weak aspect of this model is that if the scraped liquid is not fully mixed with the bulk, but a portion of it returns to the cooling surface by bypassing the scraping blade (Figure 7), this may reduce the value of the heat-transfer coefficient predicted by Eq. 19.

Heat transfer on the scraped surface with phase change (stage III)

Ice formation may occur if the temperature of the solution decreases to a certain degree of supercooling. Phase transition can be triggered by either alien particles or the addition of ice seeds, or even by some physical stimulation such as ultrasonic or mechanical vibration. Moreover, spontaneous nucleation occurs if the temperature is low enough. Once the phase transition is initiated, the latent heat released will increase the liquid temperature until it approaches the freezing point, T_f. Compared to other stages of the operation, this nucleation–temperature-rising period (that is, stage II in Figure 2) is short, from 10 s to a couple of minutes, depending on the volume of the liquid and the strength of agitation. The heat transfer during this period is unsteady. The experimental and modeling study of the heat transfer of stage II is presented in another article (Qin et al., 2002). In the rest of this article, we will focus attention on analyzing the heat transfer in stage III. An outstanding issue of this stage is that there are existing ice particles in the liquid, and the bulk temperature is very close to the freezing point, T_f , and can be approximately considered a constant.

On the subcooled metal surface, which provides a more favorable place for ice growth than the bulk solution, nucleation and crystallization of ice may take place continuously because of the collision of the ice particles. Considering that a scraping blade has just passed over the cooling surface, all the attached ice particles have been wiped off together with the liquid layer, which was replaced by a new liquid layer containing ice particles, we can assume that a new round of nucleation and crystallization of ice proceeds on it until the next scraping. This is somewhat like raindrops hitting the windscreen of a car, and then being wiped off by the windscreen wiper, as shown in Figure 8.

It is obvious that at a definite instant of time, the temperature at each small element of area is different due to the random occurrence of ice nucleation, which releases latent heat to increase the local temperature. The temperature at a selected spot should reasonably undergo and repeat the following steps: temperature increase due to the ice growth over it → temperature decrease after the scrape blade passes over. Since the temperature is uncertain at an arbitrary instantaneous time for every point of the cooling surface, only the "average temperature" over the entire surface at an instantaneous time makes sense. Therefore, in the following analysis (if not indicated), the cooling surface temperature, T_w, and the interior temperature, T, both denote the average temperature in the appropriate cross sections.

When the ice layer grows thicker to form an ice cake (this can occur if the scraper is not applied or the scrape circle is much longer than that which formed an ice cake), the temperature profile inside the ice phase and the liquid phase, and the perpendicular growth rate of the ice layer, can be described by the classic *Neumann problem* (Lunardini, 1991) for pure water. For an aqueous solution, the coupling of heat and mass transfers, which is governed by the concentration polarization, should be taken into consideration (Ratkje and Flesland, 1995; Chen et al., 1997). However, these are not in the focus of this article. What we are concerned with is the heat transfer under the circumstances where patches of ice layers have formed but not yet completely covered the entire subcooled surface.

Let us assume that the entire subcooled surface has an average temperature, T_w, at an arbitrary instant of time. The ice formation rate on it is proportional to some power of the wall supercooling

$$\frac{dM_{\text{ice}}}{dt} = k_i A (\Delta T_w)^n \qquad \text{(kg/s)}, \tag{21}$$

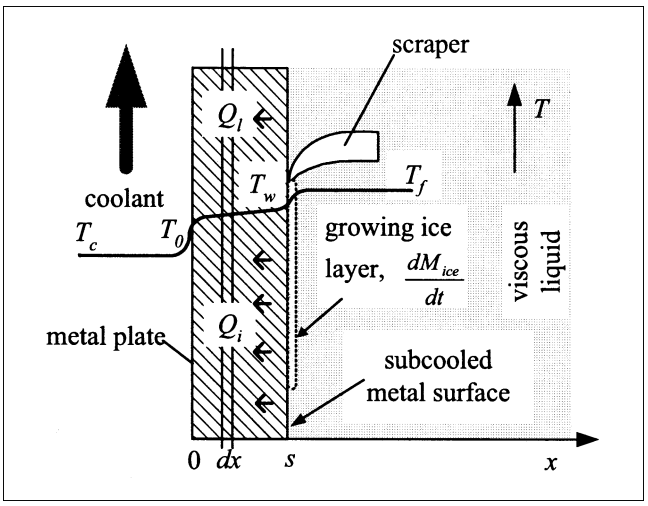

Figure 9. Cross-sectional profile of the average temperature in the metal plate.

where ΔT_w ($= T_f - T_w \approx T_b - T_w$, because the bulk temperature, T_b, is very close to the freezing point temperature, T_f) is the average wall supercooling; k_i is the constant of the mass formation rate of ice layers spreading on the subcooled surface; and A is the surface area. Ice formation in water or solutions, as reviewed and introduced by Fletcher (1970), has been studied by many researchers. Although the nucleation rate was found to be proportional to the 2.5th power of the supercooling (ΔT_w), and the linear growth rate was found to be inversely proportional to the radius of an individual ice particle (Omran and King, 1974), these rates are still unable to give the total mass formation rate of ice, especially if the ice is formed by spreading on the subcooled surface. As to the total mass formation rate of ice, according to our studies, which will be presented in another article, the value of n is very close to 1 (Qin et al., 2002). Thus, the heat generation rate due to ice formation is

$$\left.\frac{dQ_i}{dt}\right|_{x=s} = -\Delta H_i \cdot \frac{dM_{\text{ice}}}{dt} = -\Delta H_i k_i A \Delta T_w, \qquad (22)$$

where ΔH_i is the latent heat of freezing water; the minus is used because the heat flux is in the opposite direction to the x-axis in Figure 9. Since the bulk temperature is very close to the freezing point, the latent heat produced at the skin surface will be given directly to wall body. The ice nucleation and crystallization generate a dynamic "hot film," which appears-disappears continuously here and there on every small area.

Another part of the heat flux is due to the transfer of sensible heat, Q_l, which is given by the liquid, into the metal wall through the ice-free area

$$\left.\frac{\partial Q_l}{\partial t}\right|_{x=s} = -\varphi \cdot h_l \cdot A \cdot \Delta T_w, \qquad (23)$$

where φ is the ratio of the ice-free area to the total scraped area [by the definition $(0 \le \varphi \le 1)$, it should have a value between 0 and 1]; h_l is the individual heat-transfer coefficient of the liquid film; subscript s represents the cooling surface (similarly hereinafter; see Figure 9). Thus, the overall heat flux at the cooling surface is

$$\begin{aligned}\left.\frac{\partial Q}{\partial t}\right|_{x=s} &= \left.\frac{\partial Q_i}{\partial t}\right|_{x=s} + \left.\frac{\partial Q_l}{\partial t}\right|_{x=s} \\ &= -k_i \Delta H_i A \Delta T_w - \varphi h_l A \Delta T_w \\ &= -(k_i \Delta H_i + \varphi h_l) A \Delta T_w. \end{aligned} \qquad (24)$$

The temperature gradient at the cooling surface is coupled with the heat flux by Fourier's law:

$$\left.\frac{dQ}{dt}\right|_{x=s} = -\lambda_w A \left.\frac{dT}{dx}\right|_{x=s}, \qquad (25)$$

where $dT/dx|_{x=s}$ is the average value of the temperature gradient at the cooling surface. Substitution of Eq. 25 into Eq. 24, after rearrangement, yields one of the boundary conditions of the heat-transfer problem with phase change at the cooling surface

$$\begin{aligned}\left.\frac{\partial T}{\partial x}\right|_{x=s} &= \left(\frac{k_i \Delta H_i}{\lambda_w} + \frac{\varphi h_l}{\lambda_w}\right) \Delta T_w \\ &= (\beta + \gamma) \Delta T_w, \end{aligned} \qquad (26)$$

where $\beta (= k_i \Delta H_i / \lambda_w)$ represents the contribution of ice formation rate to the temperature gradient in the jacket wall; $\gamma (= \varphi h_l / \lambda_w)$ represents the contribution of the heat-transfer rate of the unfrozen liquid film to the temperature gradient in the jacket wall; and $\Delta T_w (= T_b - T_w = T_f - T_w)$ is the average degree of supercooling at the cooling surface.

On the other side of the jacket wall, assuming that the coolant flow is large enough to maintain a constant wall temperature, T_0, this gives another boundary condition of the problem shown by Eq. 27

$$T|_{x=0} = T_0. \qquad (27)$$

Note the concept of average temperature for a cross section is used in the metal plate. Since the heat extracted from the lefthand side is balanced by the heat input on the righthand side shown by Figure 9, and there is no heat source inside it, the heat transfer across the metal plate is a quasi-steady-state, yielding $(\partial T/\partial t)_{\text{III}} = 0$. (This was proved experimentally, as shown in Figures 2b and 3b.) Therefore, this one-dimensional heat transfer inside the metal plane can be written in the form of *Laplace's equation*

$$\frac{\partial^2 T}{\partial x^2} = 0. \qquad (28)$$

The heat-transfer problem presented by Eqs. 26, 27, and 28 can be solved by integrating Eq. 28 twice, and using the

boundary conditions shown by Eqs. 26 and 27

$$T = (\beta + \lambda)\Delta T_w x + T_0. \tag{29}$$

Obviously, the temperature profile inside the metal plate is linear. In order to obtain the expression of the average heat-transfer coefficient, the following definition of it is used

$$\overline{h}_{il} = \frac{1}{A\Delta T_w} \cdot \left| \frac{\partial Q}{\partial t} \right| \tag{30}$$

where $\partial Q/\partial t$ is negative because the heat flux is in the opposite direction to the x-axis. Differentiation of Eq. 29 against x gives

$$\frac{\partial T}{\partial x} = (\beta + \gamma)\Delta T_w. \tag{31}$$

According to the differential form of Fourier's law, in the metal plate, there is

$$\frac{\partial Q}{\partial t} = -\lambda_w A \frac{\partial T}{\partial x}. \tag{32}$$

Substitution of Eqs. 32 and 31 into Eq. 30 yields

$$\overline{h}_{il} = k_i \Delta H_i + \varphi h_l. \tag{33}$$

Note that the individual heat-transfer coefficient, $\overline{h}_{il}$, with phase change at the cooling surface and presented by the preceding equation, is an average value over the entire surface at a definite instant of time. Considering the average value over the time interval of a scrape circle, $\overline{h}_l$, given by Eq. 19 must be used to substitute h_l in Eq. 33. Therefore, a comprehensive expression of the individual heat-transfer coefficient at an SSHE can be written as

$$h_{il} = \begin{cases} \left(\dfrac{\lambda_l \rho_l c_{pl} nF}{15\pi} \right)^{1/2}, & \text{(without phase change)} \quad (19) \\ k_i \Delta H_i + \varphi \left(\dfrac{\lambda_l \rho_l c_{pl} nF}{15\pi} \right)^{1/2}, & \text{(with phase change)} \quad (34) \end{cases}$$

where k_i is the ice formation rate constant on the subcooled surface ($\mathrm{kg \cdot m^{-2} \cdot {}^{\circ}C^{-1} \cdot s^{-1}}$) defined by Eq. 21; ΔH_i is the latent heat of freezing, or 334.11×10^3 $\mathrm{J \cdot kg^{-1}}$ for water; λ_l, ρ_l, and c_{pl} are thermal conductivity ($\mathrm{J \cdot m^{-1} \cdot {}^{\circ}C^{-1} \cdot s^{-1}}$), density ($\mathrm{kg \cdot m^{-3}}$), and specific heat capacity ($\mathrm{J \cdot kg^{-1} \cdot {}^{\circ}C^{-1}}$) of the liquid, respectively; n and F are the rotational speed (rpm) and blade number of the scraper, respectively; φ is the ratio of the ice-free area to the entire scraped surface area ($0 \le \varphi \le 1$).

Discussion

As mentioned before, the first term $k_i \Delta H_i$ in Eq. 34 is related to the latent heat contribution to the individual heat-transfer coefficient, and the second term is related to the sensible heat contribution. When the wall temperature is above the freezing point (that is, $\Delta T_w \le 0$), there is no ice formation on it, so $k_i = 0$ and $\varphi = 1$, leading to the retrieval of Eq. 19. However, when the degree of supercooling at the cooling surface is positive ($\Delta T_w > 0$) to begin forming ice, the latent heat of freezing will directly transfer into the cooling surface. Note that the value of latent heat is much greater than the sensible heat, for example, in the case of water, 80 times as much energy is released to freeze 1 kg of water than to lower the temperature of 1 kg of water by 1°C. This results in a step increase of the heat-transfer coefficient, h_{il}, because of the sudden appearance of the first term, $k_i \Delta H_i$. Moreover, the increase in the heat-transfer coefficient is maintained by scraping the newly formed ice off continuously; otherwise, the heat transfer will be damped after the ice layer spreads over the entire cooling surface.

The ratio φ of the ice-free area to the entire cooling area, by its definition, will decrease after the onset of ice formation (Qin et al., 2002). However, the first term, $k_i \Delta H_i$, in Eq. 34 does not change with the degree of supercooling. This results in the existence of a maximum h_{il} when the wall supercooling, ΔT_w, is just large enough to start ice formation spreading on the cooling surface, and explains the experimental results shown in Figure 4.

When the concentration of the aqueous solution increases, the influence of the viscosity on the ice formation rate gradually becomes important, which reduces the ice formation rate, especially when a crystallization inhibitant, such as protein, surfactant, emulsified fat, or starch, are present to form a viscous liquid. This can be found in the production of ice cream or in the late stage of freeze concentration when solutions become very thick. An extreme situation is when the aqueous liquid has become so thick and viscous (or the crystallizable free water has become so scarce), that the ice formation rate at the subcooled metal surface tends to be zero, that is, $k_i \to 0$, and $\varphi \to 1$. The heat-transfer pattern finally reverts back to Eq. 19 again.

The experiments on whole-milk freeze concentration in this study showed that the heat-transfer coefficient achieved a maximum when the supercooling on the scraped surface is in the range of 0.3–0.6°C. As shown in Figure 4, a further increase in the wall supercooling would reduce the heat-transfer coefficient, even though ice scraping was used.

Although we have been trying to correlate the thermal properties of the jacket wall, such as its thermal conductivity, λ_w, density, ρ_w, and specific heat, c_{pw}, with the expression of the heat-transfer coefficient, they are all absent in Eq. 34 at the end. A further study of the growth kinetics of ice layers spreading on a subcooled surface has shown that k_i is a function of λ_w, ρ_w, and c_{pw}, which means the thermal properties of the cooling jacket influence the heat-transfer coefficient by impacting the phase transition rate at a subcooled SSHE. This will be presented in another article.

Conclusions

Three typical heat-transfer patterns were identified during the process of freeze concentration in an SSHE. They correspond to the stages of chilling, nucleation, and crystallization, respectively. These processes can also be found in the pro-

duction of ice cream. Experimental measurement of a subcooled SSHE showed that there was a step increase in heat transportation at the onset of ice formation. The overall heat-transfer coefficient of stage III was found to be 415 ($Wm^{-2}\cdot°C^{-1}$), about 1.5 times larger than that of stage I, which was 275 ($Wm^{-2}\cdot°C^{-1}$) in this study. Even though the ice formation on the cooling surface can be considered disadvantageous to the heat transfer, experimental analysis showed that the direct liberation of the latent heat of ice crystallization on the cooling surface actually "boosts up" heat transference.

Under the continuous surface-scraping condition, the unsteady heat transfer of stages I and III can be converted to the problems of quasi-steady-state heat transfer by averaging the heat-transfer rate over the time interval of a scrape circle, and over the entire scraped surface. Mathematical derivation of the problem has arrived at a unified expression of the heat-transfer coefficient for the subcooled SSHE with or without phase change. The model predicts (1) a step increase in heat transfer occurs when the phase change commences, and (2) a maximum heat-transfer coefficient exists in a narrow range of the wall supercooling after the freezing point is reached. These predictions are consistent with the experimental results during freeze concentration in this study. The model also demonstrates the relationship of the heat transfer between stage I and stage III.

Notation

A = heat-transfer area, m^2

c_{pl} = specific heat of the liquid (whole milk in this study), $J\cdot kg^{-1}\cdot°C^{-1}$

c_{pw} = specific heat of the wall material, $J\cdot kg^{-1}\cdot°C^{-1}$

C_1, C_2 = initial and final concentrations of the liquid during freeze concentration, kg solute/kg liquid

F = blade number of the scraper

ΔH_i = latent heat of freezing of water, (334.11×10^3 $J\cdot Kg^{-1}$), $J\cdot kg^{-1}$

h_c = individual heat-transfer coefficient of the coolant, $W\cdot m^{-2}\cdot°C^{-1}$

$\bar{h}_l$ = average individual heat-transfer coefficient of the liquid on the scraped-surface heat exchanger without phase change, $W\cdot m^{-2}\cdot°C^{-1}$

$\bar{h}_{il}$ = average individual heat-transfer coefficient of liquid and ice on the subcooled-scraped surface with phase change, $W\cdot m^{-2}\cdot°C^{-1}$

k_i = constant of ice formation rate on the scraped-subcooled surface, $kg\cdot m^{-2}\cdot°C^{-1}\cdot s^{-1}$

M_m,M_{ice} = liquid (such as milk) mass, and pure ice mass, respectively, kg

n = (1) rotational speed of the scraper; (2) power of supercooling $(\Delta T_w)^n$, rpm

Q = heat, J

Q_τ = heat transfer in the time interval of a scraping circle, J

Q_l = heat input to the wall surface from liquid on ice-free area, J

Q_i = heat input to the wall surface directly given by the talent heat of ice formation, J

T_b = bulk temperature of the liquid, °C

T_f = freezing temperature of the liquid, °C

T_m,T_c = liquid (milk in this study), and coolant temperature, °C

T_0,T_w = surface temperature of the jacket wall at the coolant side and liquid side, respectively, °C

ΔT_w = degree of supercooling at the cooling surface ($\Delta T_w = T_f - T_w$), °C

U = overall heat-transfer coefficient, $W\cdot m^{-2}\cdot°C$

U_{I},U_{III} = overall heat-transfer coefficient in stage I and stage III, respectively, $W\cdot m^{-2}\cdot°C$

t = time elapsed after the scraping action, s

v = growth rate of ice layer spreading on the cooling surface, $m\cdot s^{-1}$ or $\mu m\cdot s^{-1}$

$z = \dfrac{x}{2\sqrt{\alpha_l t}}$ = variable introduced by *Bolzmann* transformation

Greek letters

$\alpha_l = \dfrac{\lambda_l}{\rho_l c_{pl}}$ = thermal diffusivity of the liquid, $m^2\cdot s^{-1}$

φ = ratio of ice-free area to the total area of the scraped surface ($0 \le \varphi \le 1$)

λ = thermal conductivity, $W\cdot m^{-1}\cdot°C^{-1}$

μ = viscosity of the liquid, $Pa\cdot s$

θ = dimensionless temperature

ρ_l = density of the liquid, $kg\cdot m^{-3}$

ρ_w = density of the wall material, $kg\cdot m^{-3}$

τ = time interval between two scrape-wiping ($= 60/nF$), s

$\beta = \dfrac{\Delta H_i k_i}{\lambda_w}$ = represents the contribution of ice formation rate to the temperature gradient on the scraped-subcooled surface

$\gamma = \dfrac{\varphi h_l}{\lambda_w}$ = represents the contribution of heat-transfer rate of the liquid film to the temperature gradient on the scraped-subcooled surface

Literature Cited

Abichandani, H., S. Sarma, and D. Heldman, "Hydrodynamics and Heat Transfer in Liquid Full Scraped Surface Heat Exchangers: A Review," *J. Food Process Eng.*, **9**, 121 (1987).

Baccar, M., and M. S. Abid, "Numerical Analysis of Three-Dimensional Flow and Thermal Behaviour in a Scraped-Surface Heat Exchanger," *Rev. Gen. Thermodyn.*, **36**, 782 (1997).

Chandarana, D. I., and J. A. Unverferth, "Residence Time Distribution of Particulate Foods at Aseptic Processing Temperatures," *J. Food Eng.*, **28**, 349 (1996).

Chen, X. D., P. Chen, and K. W. Free, "A Note on the Two Models of Ice Growth Velocity in Aqueous Solutions Derived from an Irreversible Thermodynamics Analysis and the Conventional Heat and Mass Transfer Theory," *J. Food Eng.*, **31**, 395 (1997).

Cuevas, R., M. Cheryan, and V. Porter, "Performance of Scraped Surface Heat Exchanger Under Ultra-High Temperture Conditions: A Dimensional Analysis," *J. Food Sci.*, **47**, 619 (1982).

Djelveh, G., and J. B. Gros, "Estimation of Physical Properties of Foamed Foods Using Energy Dissipation in Scraped-Surface Heat Exchangers," *J. Food Eng.*, **26**, 45 (1995).

Fletcher, N. H., *The Chemical Physics of Ice*, Cambridge Univ. Press, London (1970).

Harrod, M., "Scraped-Surface Heat Exchangers," *Food Process. Eng.*, **9**, 62 (1986).

Holman, J. P., *Heat Transfer*, McGraw-Hill, New York (2002).

Lunardini, V. J., *Heat Transfer with Freezing and Thawing,* Elsevier, Amsterdam and New York (1991).

Omran, A. M., and C. J. King, "Kinetics of Ice Crystallization in Sugar Solution and Fruit Juices," *AIChE J.*, **20**, 795 (1974).

Qin, F. G. F., A. B. Russell, and X. D. Chen, "Experimental Study of Ice Fouling on the Subcooled Metal Surfaces," *Asian Pacific Confederation of Chemical Engineering (APCChE) and 30th Annual Australasian Chemical Engineering Conf. (CHEMECA)*, Univ. of Canterbury, Christchurch, New Zealand (2002).

Qin, F. G. F., X. D. Chen, J. Z. Zhao, A. B. Russell, J. J. Chen, and L. Robertson, "Modeling of the Unsteady Heat Transport in the Onset Time of Nucleation and Crystallization of Ice from the Subcooled Solution," *Proc. Asian Pacific Confederation of Chemical Engineering (APCChE) and 30th Annual Australasian Chemical Engineering Conf. (CHEMECA)*, Univ. of Canterbury, Christchurch, New Zealand (2002).

Ratkje, S. K., and O. Flesland, "Modelling the Freeze Concentration Process by Irreversible Themodynamics," *J. Food Eng.*, **25**, 553 (1995).

Zheng, L., A. B. Russell, and D. I. Wilson, "Influence of Crystallisation on Heat Transfer Through a Scraped Surface," *Proc. World Congress of Chemical Engineering*, The Univ. of Melbourne, Melbourne, Australia, (2001).

Appendix: Derivation of the Solution of the Heat-Transfer Partial Differential Equation

Rewrite Eqs. 8–11

$$\begin{cases} \dfrac{\partial T}{\partial t} = \alpha \dfrac{\partial^2 T}{\partial x^2} & \text{(A1)} \\ T(x,0) = T_b & \text{(A2)} \\ T(0,\, t) = T_w & \text{(A3)} \\ T(\infty,\, t) = T_b. & \text{(A4)} \end{cases}$$

Introduce a new variable

$$z = \frac{x}{2\sqrt{\alpha t}}, \tag{A5}$$

which is also known as the Boltzmann transformation (Lunardini, 1991), and define a dimensionless temperature

$$\theta = \frac{T - T_w}{T_b - T_w} = f(z). \tag{A6}$$

The initial and boundary conditions given by Eqs. A2–A4 become

$$\begin{cases} \theta(x,0) = 1 & \text{(A7)} \\ \theta(0,t) = f(0) = 0 & \text{(A8)} \\ \theta(\infty,t) = f(\infty) = 1. & \text{(A9)} \end{cases}$$

Differentiation of θ against t gives

$$\frac{\partial \theta}{\partial t} = \frac{1}{T_b - T_w}\frac{\partial T}{\partial t} = \frac{df}{dz}\frac{\partial z}{\partial t} = -\frac{xt^{-3/2}}{4\sqrt{\alpha}}\frac{df}{dz} \tag{A10}$$

$$\frac{\partial \theta}{\partial x} = \frac{1}{T_b - T_w}\frac{\partial T}{\partial x} = \frac{df}{dz}\frac{\partial z}{\partial x} = \frac{1}{2\sqrt{\alpha t}}\frac{df}{dz} \tag{A11}$$

$$\frac{\partial^2 \theta}{\partial x^2} = \frac{1}{T_b - T_w}\frac{\partial^2 T}{\partial x^2} = \frac{d}{dz}\left(\frac{1}{2\sqrt{\alpha t}}\frac{df}{dz}\right)\frac{\partial z}{\partial x} = \frac{1}{4\alpha t}\frac{d^2 f}{dz^2}. \tag{A12}$$

Substitution of $\partial T/\partial t$ and $\partial^2 T/\partial x^2$ from Eqs. A11 and A12, into Eq. A1, yields

$$\frac{d^2 f}{dz^2} + 2z\frac{df}{dz} = 0. \tag{A13}$$

Letting $P = (df/dz)$, Eq. A13 becomes

$$P' + 2zP = 0. \tag{A14}$$

Its general solution is

$$P = \frac{df}{dz} = C_1 e^{-z^2}. \tag{A15}$$

Therefore

$$f(z) = \int_0^z C_1 e^{-z^2} dz + C_2. \tag{A16}$$

Applying the boundary conditions given by Eqs. A8 and A9, we can get

$$C_2 = 0 \tag{A17}$$

$$C_1 = \frac{1}{\displaystyle\int_0^\infty e^{-z^2} dz} = \frac{2}{\sqrt{\pi}}. \tag{A18}$$

Therefore the solution of Eq. A1 is

$$f(z) = \frac{T - T_w}{T_b - T_w} = \frac{2}{\sqrt{\pi}}\int_0^z e^{-z^2} dz. \tag{A19}$$

Manuscript received Oct. 1, 2002, and revision received Feb. 18, 2003.